



## 1    **1. Introduction**

2    The most common methodology applied currently to check the ultimate limit state of static equilibrium (SEQ) of masonry  
3    historical structures is based on the application of the limit analysis criterion developed by Heyman [1] after the numerical  
4    or graphical resolution of the structural equilibrium equations system. It is based on a comparative study between the  
5    equilibrium situation of the structure and its limit situation considering the stability. The result of that study is the  
6    geometrical factor of safety [1] as an indicator of the safety of the structure considering its stability when any combination  
7    of loads is applied and fixed supports are considered at its foundation. The equilibrium situation of the structure, applying  
8    this methodology, is determined considering the equilibrium equations, but not the compatibility and the material  
9    constitutive equations and therefore, the calculated result only depends on the geometry of the structure, the applied loads  
10   and the reactions considered at its supports. This methodology assumes the following hypothesis [1]:

- 11        • The masonry blocks are rigid elements and it is assumed that the material failure is not possible in  
12                compression.
- 13        • The masonry tensile strength is null. The cohesion due to the mortar located between blocks is not considered.
- 14        • The sliding between blocks is not possible.

15   The graphical representation of the equilibrium equations system solution is the funicular polygon that equilibrates the  
16   applied loads on the structure. From this polygon can be deduced the thrust line that allows knowing the minimum  
17   dimensions of the structure that are necessary to be in situation of static equilibrium and comparing them with the actual  
18   dimensions of the structure, the geometrical factor of safety can be determined. It is considered by Heyman [2] that a  
19   masonry historical structure is safe, in terms of stability, when its geometrical factor of safety is equal or higher than 2.

20   An essential aspect in the numerical simulation of historical structures concerns the constitutive laws that define the  
21   material behaviour. On this respect, different papers can be found in the specialized literature. So, different authors focus  
22   their research on the development of constitutive laws for masonry and the interfaces (Benedetti [3], Lourenco [4]). Other  
23   authors use specific constitutive laws in the finite element simulations (Dhanasekar [5], Giordano [6], Kishi [7]).

24   In the experimental field, some authors have applied different techniques for the strength assessment of de masonry walls  
25   (Binda [8], Corradi [9]). Other authors apply experimental techniques for the structural integrity assessment (Ercan [10]).

26   Most of the published works are focused on the structural integrity after seismic effects (Betti [11], Castellazi [12],  
27   Corradi [13], de Luca [14], Kishi [7], Mallardo [15]) in order to evaluate firstly the damage induced by the earthquake,  
28   and then to study reinforcement solutions that allow recovering the stability and functionality if possible. Most of these  
29   works (Betti [11], Castellazi [12], Mallardo [15], Modena [16], Valluzzi [17]) deal with the study of huge monumental  
30   buildings like churches, cathedrals, aqueducts, etc., by using experimental techniques (Valluzzi [17]), computational

1 models based on the finite element method (Betti [11], Castellazi [12], Modena [16], Valluzzi [17]), or a combination of  
2 both (Ercan [10]).

3 Concerning structural analysis, in the situations where the hypotheses that are assumed by the limit analysis criterion are  
4 not satisfied, the ultimate limit state of structural resistance (STR) should be checked. The most common methodology  
5 applied currently to check this ultimate limit state of masonry historical structures is based on the application of the FEM  
6 based approaches described by Roca [18] which take into account the equilibrium, compatibility and material constitutive  
7 equations and therefore, they also allow checking the ultimate limit state of SEQ in these particular situations although not  
8 to know the geometrical safety factor of the structure. E.g. a macro-model was used by Roca [19] in the analysis of the  
9 Küçük Ayasofya Mosque in Istanbul and a micro-model was used by Lourenço [20] in the analysis of masonry shear  
10 walls. A widespread review concerning the different techniques used for analyzing and repairing historical structures can  
11 be found in Roca [18].

12 The majority of works applying FEM to historical structures are devoted to evaluate the damage induced by earthquakes,  
13 and then to study reinforcement solutions that allow recovering the stability and functionality. Besides that, other authors  
14 analyze the structural behaviour of historical structures under different conditions. So, in Del Coz [21] a study of the  
15 structure of the chapel of San Salvador de Valdediós (Spain) and proposals for its restoration are presented, considering  
16 the severe damage detected in the chapel vault. The Romanesque Farneta abbey (Italy) is analyzed in Betti [22] in order to  
17 assess the effectiveness of the usual structural reinforcement in terms of increased the seismic capacity. In Romera [23,  
18 24] the Basilica of Pilar (Spain) is analyzed by means of a set of structural models of the entire temple and local models of  
19 the Regina Martirum dome identifying the actual structural state of the church, its safety level and the relationship  
20 between the structural behaviour and the damages observed. A study on the bell tower of the Church of Santas Justa and  
21 Rufina (Spain) is carried out in Ivorra [25] to predict the evolution of its dynamic behaviour in relation to subsidence  
22 caused by variations in the level of the water table during periods of drought. Finally, the static behaviour and the seismic  
23 vulnerability of the Basilica of Santa Maria all'Impruneta (Italy) are analyzed in Betti [26], evaluating the capacity of the  
24 church to withstand lateral loads together with the expected demands resulting from seismic actions.

25 In this context, the aim of this work is the assessment of the Saint Sebastian church, located in Piedratjada (Zaragoza,  
26 Spain), in which were currently detected several cracks, which could be due the soil settlement. In a first step, the  
27 structure is analyzed in normal conditions; in the second step, the influence of soil settlement effects are analyzed,  
28 determining its maximum admissible value; finally, in the third step, a couple of reinforcement solutions are studied in  
29 order to guarantee the requested structural safety in the long term. The Eurocode criteria have been considered for the  
30 structural assessment.

31

1     **2. Material and Methods**

2     **2.1 Description of the assessed church and current pathologies**

3     The Saint Sebastian church, located in Piedratajada (Zaragoza, Spain), was built based on the romanesque architecture  
4     style in the 14<sup>th</sup> century and it suffered a refurbishment in the 16<sup>th</sup> century, when its roof was removed and it was built  
5     again based on the gothic architecture style. The church was restored in 1990 in order to improve its appearance but new  
6     cracks have been detected currently. The origin of these pathologies appears to be the soil settlement shown in Fig. 1,  
7     which was detected at the west area of the church. Consequently, a portal frame of the structure has been assessed in order  
8     to check the current safety level of the structure in the affected area according to the Eurocodes and to propose the optimal  
9     reinforcement of the structure if it will be necessary to increase its reliability.



10  
11     **Fig. 1.** The west view of the St. Sebastian Church

12

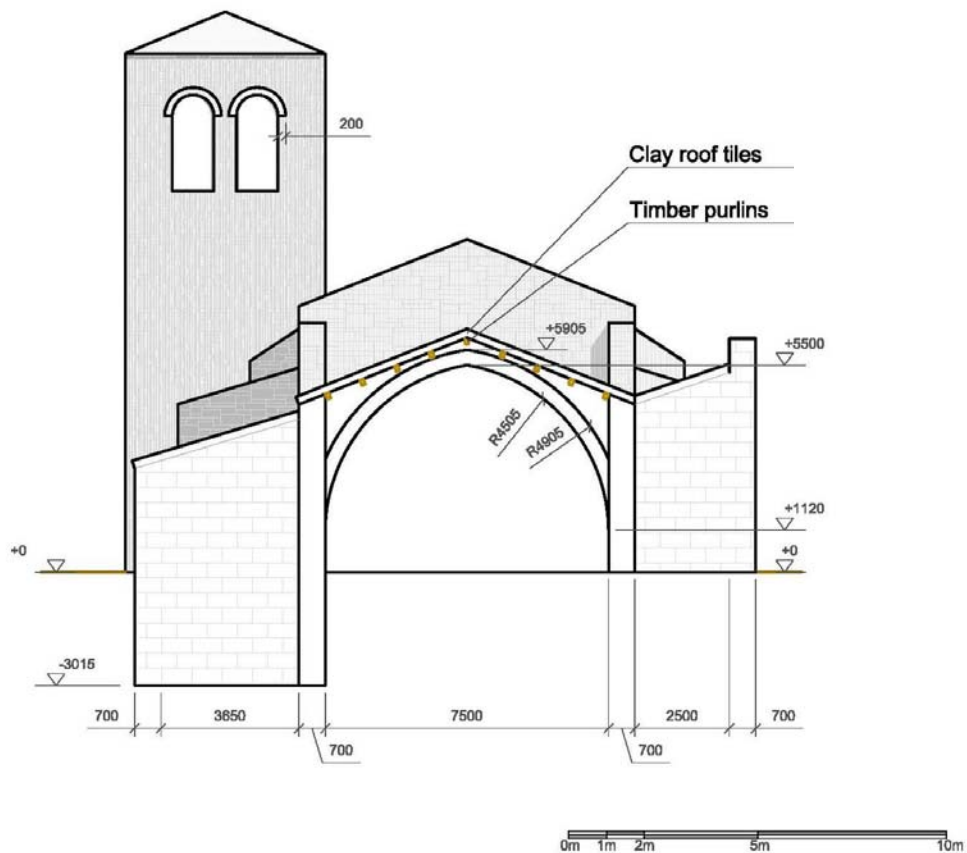
13     **2.2 Methodology basis**

14     The proposed methodology in this work for the assessment of masonry historical structures as the Saint Sebastian church,  
15     is based on the analysis of a discontinuous FEM model created under a particular criterion which allows checking both the  
16     ultimate limit state of SEQ through the geometrical factor of safety and the ultimate limit states of STR and soil bearing  
17     capacity (SBC), according to the Eurocodes, under the consideration of the following hypotheses:

- 18     • There is no tensile strength at the joints between blocks
- 19     • The shear strength of the masonry is limited by the tensile strength of the blocks (masonry units) and the static  
20     frictional coefficient in the contact surfaces between blocks.
- 21     • The brittle failure of the blocks occurs in tension as the elastic limit in tension is reached.
- 22     • Plastic deformation and crushing appear as the elastic limit in compression of the masonry is reached.

1     **2.3 Geometric model**

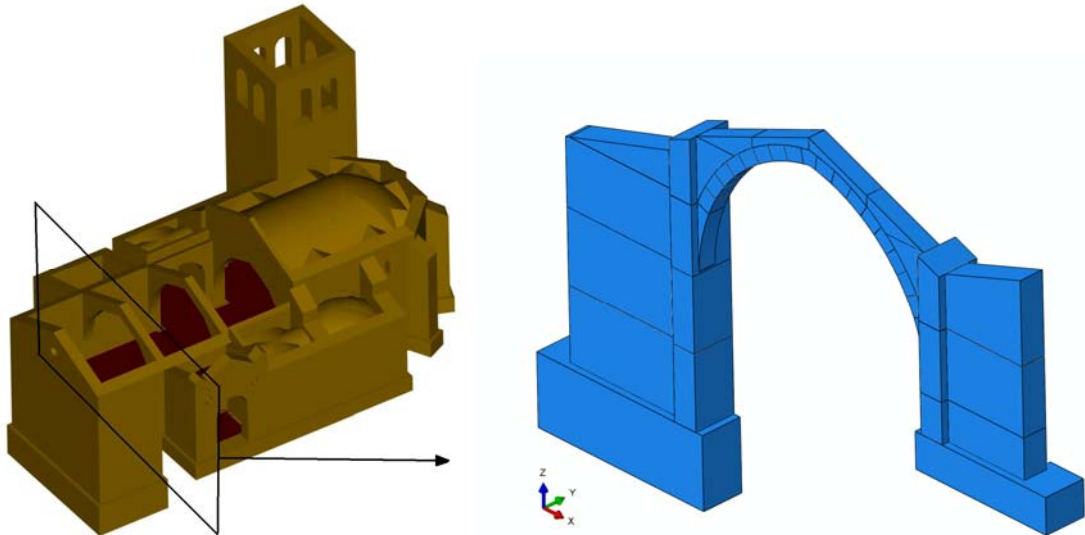
2     The dimensions of the assessed portal frame are shown in Fig. 2. They have been used to create the geometric model of  
3     the church which represents the “design” shape of the historical construction, not the current shape that is affected by the  
4     execution tolerances and the action of loads or settlements. This geometric model has been created with a CAD  
5     application as shown in Fig. 3, where one of the portal frames of the west area is extracted from the whole geometric  
6     model to be analysed applying the proposed methodology. The posterior part of the church, which is affected by the  
7     observed pathologies, is composed by two independent frames and the posterior wall. Timber purlins of wood are  
8     arranged over the frames supporting wooden flooring. Finally, clay roof tiles are disposed over the wooden flooring.  
9     Building enclosure is made from sandstone not interwoven with the frame but connected by a mortar joint. So, the 3D  
10    effect is negligible, allowing modelling a single frame. The parts which have a clearly three-dimensional behaviour (barrel  
11    vault and tower) are not affected currently by the pathology.  
12    The portal frame marked in Fig. 3 (the most affected by the pathology) is divided in pieces in order to determine the  
13    geometrical factor of safety of the structure (SEQ checking) and to check adequately the masonry structural resistance  
14    (STR checking) in the analysis exposed above. Those divisions are based on the cut criterion described in Ayensa [27].



15

16

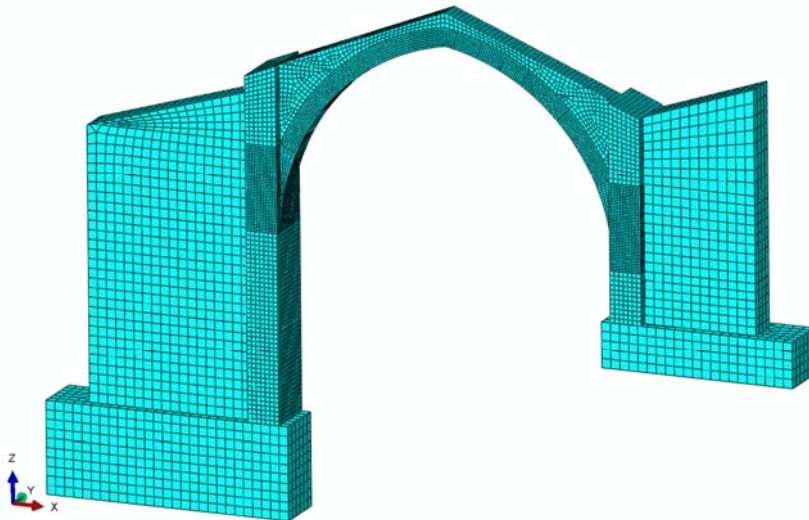
**Fig. 2.** The assessed portal frame of the St. Sebastian church (dimensions in mm)



1  
2 **Fig. 3.** The geometric model and the assessed portal frame of the St. Sebastian church

3  
4 **2.4 Finite element model**

5 The tasks described above were performed to prepare the discontinuous FEM model to be analysed in Abaqus 6.11 [28]  
6 applying the finite element method. Each piece of the portal frame shown in Fig. 3 is meshed with quadratic brick  
7 elements of 20 nodes defined as “C3D20R” in Abaqus [28], which maximum size is 50 mm for the pointed arch, 100 mm  
8 for the piers and the masonry over the arch and 200 mm for the walls and the foundations, respectively. After that, the  
9 meshed pieces are assembled as shown in Fig. 4.



10  
11 **Fig. 4.** The portal frame meshed to be analysed in Abaqus

12  
13 **2.5 Material properties**

14 The material properties have been determined applying the equations 1 to 5 with the parameters obtained from the study  
15 of the building “on site” and using specialized bibliography. The properties of the material are:

- Masonry density: 23 kN/m<sup>3</sup>, according to bibliography (Baker [29] used a value of 23 kN/m<sup>3</sup>; Betti, 2012 [11] and Ercan [10] used a value of 21 kN/m<sup>3</sup>; Giordano [6] used a value of 25 kN/m<sup>3</sup>) for sandstone blocks and very thin bed joints of poor mortar between them.
- Masonry Young's modulus: 10200 MPa, calculated according to the UIC [30] expression:

$$E = E_b \cdot \frac{1 + \alpha}{1 + \alpha \cdot \beta} \quad (1)$$

where  $E_b = 20000$  MPa, according to Baker [29] (values between 10000 and 50000 MPa are recommended for sandstone in [30], depending on the sandstone origin; a mean value of 15500 MPa, with values raising 20300 MPa, is reported more recently in Oliveira [31] for a kind of stone similar to the used in the analyzed church);  $\alpha = 0.02$  and  $\beta = 50$  are two parameters that represents the following relationships:

$$\alpha = \frac{h_m}{h_b} \quad \beta = \frac{E_b}{E_m} \quad (2)$$

where  $h_b$  is the average height of the sandstone blocks,  $h_m$  is the average thickness of the poor mortar bed joints,  $E_b$  is the Young's modulus of the blocks and  $E_m$  is the Young's modulus of the poor mortar. Different analyses with values of  $E_b$  in the range 16000-24000 MPa (-/+ 20%) were performed to verify the influence of the Young's modulus in the structural behaviour of the frame.

- Long term Young's modulus of masonry: 5100 MPa, calculated according to the following expression of the Eurocode 6 [32]:

$$E_{longterm} = \frac{E}{1 + \varphi} \quad (3)$$

where  $\varphi=1$  is the final creep coefficient for masonry units of stone.

- Masonry Poisson's ratio: 0.2 as is usual for sandstone masonry structures (Riddington [33]; Betti 2012 [11]; Giordano [6]).
- Design value of the masonry compressive strength: 5 MPa, calculated with equation 4, adapted from the formula of Ohler [34]:

$$f_k = \frac{\alpha \cdot f_{b,k}}{1 + 10 \cdot b \cdot \alpha} \quad f_d = \frac{f_k}{\gamma_R} \quad (4)$$

where  $\gamma_R=3$  is the partial factor for the masonry compressive strength recommended by the Eurocode 6 [32] for a masonry structure composed by stone blocks and bed joints of poor mortar,  $f_{b,k}=22$  MPa is the characteristic compressive strength of the sandstone blocks (minimum value was selected according to Baker [29]; a value of

40 MPa is used in Betti [26]; mean values over 50 MPa were obtained by Oliveira in experimental compression tests [31]) and both 'a' and 'b' are non-dimensional parameters that depend on  $\alpha$  (Table 1).

**Table 1.** Parameters of the Ohler formula

	a	b
$\alpha \leq 0,02$	1.00	2.22
$0,02 < \alpha < 0,05$	0.81	0.96
$\alpha \geq 0,15$	0.66	0.66

- Design value of the axial tensile strength of the blocks: 0.4 MPa, calculated with equation 5:

$$f_{b,tk} = 0.05 \cdot f_{b,k} \quad f_{b,td} = \frac{f_{b,tk}}{\gamma_R} \quad (5)$$

- Material failure properties: defined as "concrete damaged plasticity" in Abaqus [28]. It is based on the design value of the masonry compressive and tensile strength and provides a capability to consider a non linear behaviour for brittle materials as concrete or stone. This criterion has offered acceptable results according to Giordano [6].

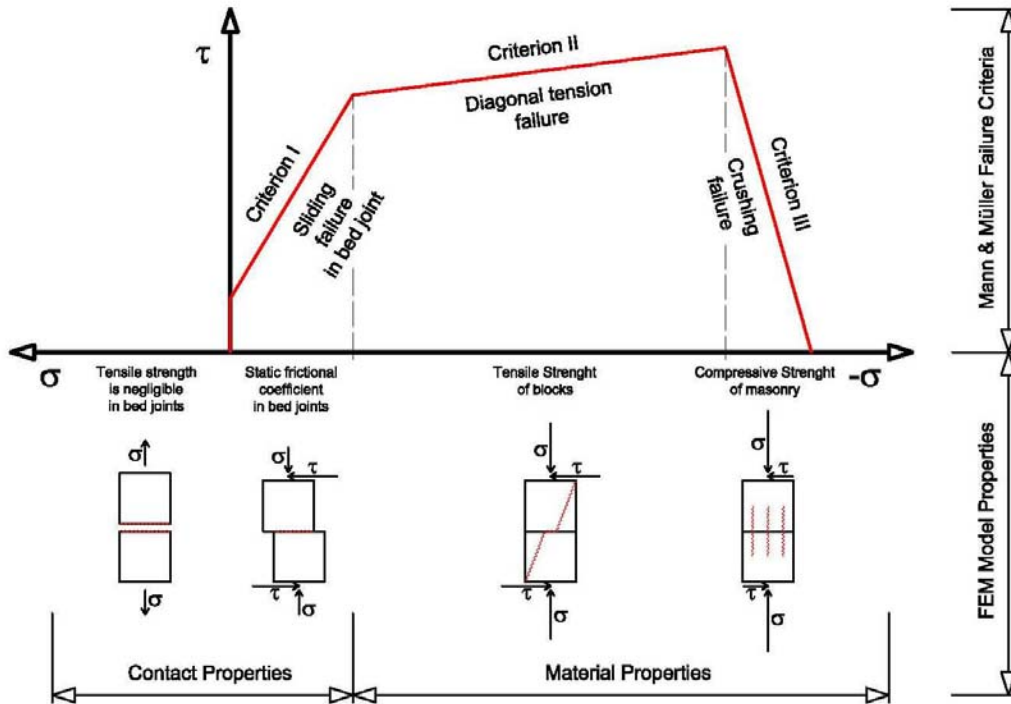


**Fig. 5.** The Mann & Müller failure criteria and its relationship with the FEM model properties

On the other hand, the following contact properties between pieces were:

- Normal behaviour: defined as "hard contact" in Abaqus [28]. It disables the possibility of interference between the pieces.



- Tangential behaviour: defined as "Lagrange multiplier" in Abaqus [28]. It allows the sliding between pieces if the maximum friction load is exceeded (a friction coefficient of 0.2 was considered).

Both the material failure properties assigned to the meshed pieces and the contact properties assigned to the contact surfaces between them, are the basis to consider the masonry failure criteria of Mann & Müller [35] (Fig. 5).

## 2.6 Loads and boundary conditions

The characteristic value of the permanent (G), variable (Q<sub>k</sub>) and accidental (A<sub>d</sub>) actions that can act on the structure are obtained from the Eurocode 1 [36], considering a return period of 100 years for the variable actions due to the climatologic loads that act on the monumental building structure which design working life category is 5 according to the Eurocode 0 [37]. The following loads have been considered: masonry self-weight (23 kN/m<sup>3</sup>); roof self-weight (1.25 kN/m<sup>2</sup>); roof maintenance (1 kN/m<sup>2</sup>); snow load (0.65 kN/m<sup>2</sup>); wind load (1.24 kN/m<sup>2</sup>, multiplied by the pressure coefficient c<sub>pe</sub> according to Eurocode 1 [36]).

Finally, the design values of the actions, used to define the combinations for persistent, transient or accidental design situations, in order to check all the ultimate limit states of the structure (SEQ, STR and SBC), were the defined by Lemaire [38] as the design point according to the First Order Reliability Method (FORM) described by Tichý [39] and considered by the Eurocode 0 [37], are obtained multiplying the safety partial factors by the representative value of the actions (Table 2). A reliability class RC3 was considered.

**Table 2.** Partial safety coefficients

Checking	Persistent situation		Accidental situation	
<b>Stability of the structure</b>	$\gamma_{G, stb} = 0,90$	$\gamma_{Q, dst} = 1,65$	$\gamma_{G, stb} = 0,90$	$\gamma_{Q, dst} = 1,32$
<b>Slidding between blocks</b>	$\gamma_{G, stb} = 0,90$	$\gamma_{Q, dst} = 1,65$	$\gamma_{G, stb} = 0,90$	$\gamma_{Q, dst} = 1,32$
<b>Masonry resistance</b>	$\gamma_G = 1,5$	$\gamma_Q = 1,65$	$\gamma_G = 1,1$	$\gamma_Q = 1,1$
<b>Reinforcement resistance</b>	$\gamma_G = 1,5$	$\gamma_Q = 1,65$	$\gamma_G = 1,1$	$\gamma_Q = 1,1$
<b>Soil bearing capacity</b>	$\gamma_G = 1,1$	$\gamma_Q = 1,1$	$\gamma_G = 1,1$	$\gamma_Q = 1,1$

Concerning boundary conditions, all nodes located at the base of the foundations are clamped if no settlement is considered or an imposed movement in the settled zone is applied.

## 2.7 Analysis steps

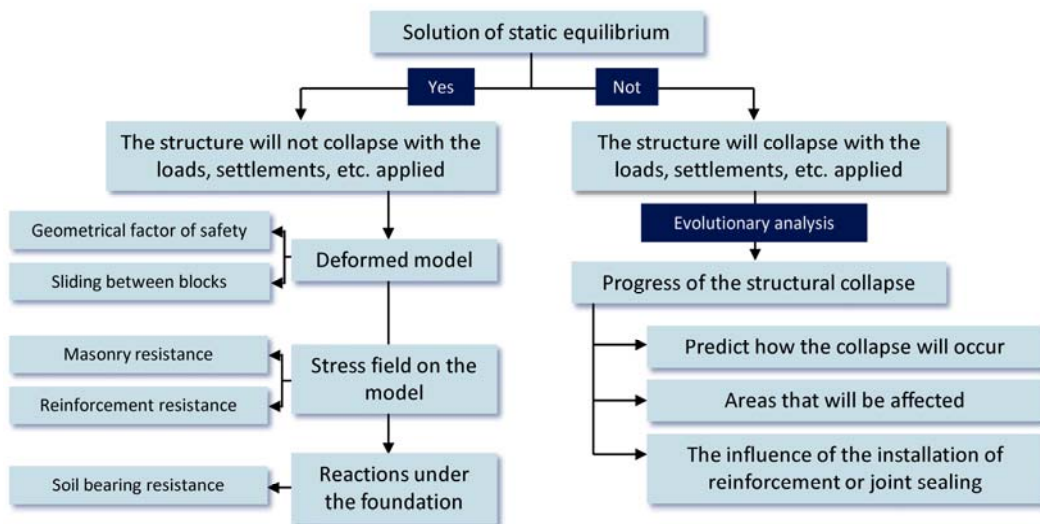
The building progress of the Saint Sebastian church was considered in the structural analysis through the definition of three analysis steps: 1) the foundations and the north wall located below the +0.00m level; 2) the walls located over the +0.00m level in conjunction with the elements existing in the previous step (starting with their initial conditions); 3)

1 finally, the pointed arch in conjunction with the elements existing in the second step (starting again with their initial  
 2 conditions). Additional steps were used for the assessment of the church considering the current foundation settlements  
 3 and the possibility of reinforcements installation.

## 5 2.8 Checking the ultimate limit states

6 Figure 6 shows the flow diagram for checking the ultimate limit states. So, the ultimate limit state of SEQ considering the  
 7 structural stability is checked by two ways. Initially is necessary to obtain a static equilibrium solution in all of the design  
 8 situations, because when an equilibrium solution exists then the collapse of the structure will not occur under the  
 9 considered boundary conditions. On the other hand, it is also necessary to determine the geometrical factor of safety  
 10 described by Heyman [1] in order to check adequately the ultimate limit state of SEQ. This factor takes into account the  
 11 uncertainty existing between the real church geometry, built with high execution tolerances (e.g. incomplete fillings at the  
 12 bed joints, imprecise geometry and so on), and the design shape of the church considered to create the geometric model.

13 This second way to check the SEQ is essential in addition to the first way, because this type of structures are characterized  
 14 by their shelf-weight as the dominant action that acts on them and its safety level considering the static equilibrium can't  
 15 be only controlled by applying the partial factors on the stabiliser and destabiliser actions. Obviously, this second way  
 16 could be avoided considering the local and global imperfections in the geometric model shape, but it would be extremely  
 17 difficult to achieve.



19 **Fig. 6.** Verifications that can be checked applying the proposed methodology

20  
 21  
 22 The geometrical factor of safety is usually deduced considering the limit analysis criteria and the solution of the  
 23 equilibrium equations of the structure. This solution can be obtained applying the graphic statics or numerical methods  
 24 and it is represented graphically by the thrust line. Instead of this procedure, this work proposes a new method to calculate

1 the geometrical factor of safety from the results obtained in the FEM analysis, based on analysing the cracks opened at the  
 2 joints between pieces in the deformed model. Usually, local geometrical factor of safety at any joint is computed  
 3 considering the ratio between the compressed area and the whole area of the contact surface. This factor should be higher  
 4 than 2 in structures as the Saint Sebastian church according to Heyman [1].

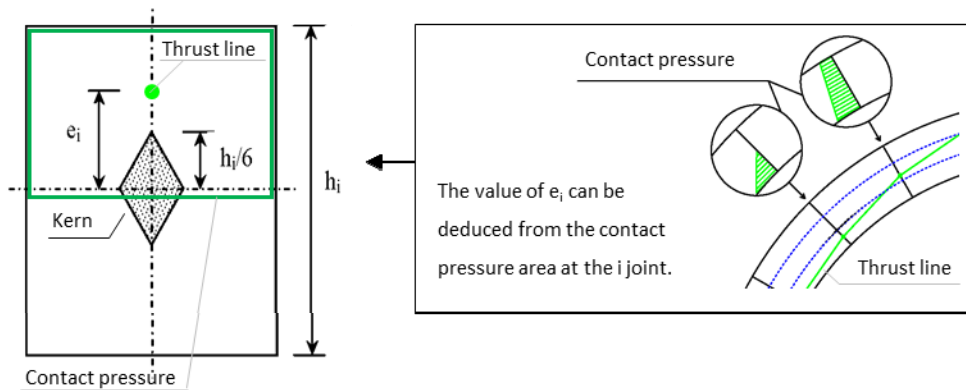
5 In the conventional procedure, three discrete values are assigned at any joint depending on the situation:  $GSF_i = 3$  when  
 6 the ratio is equal to 1,  $GSF_i = 2$  when the ratio is equal to 0.75 and  $GSF_i \approx 1$  when the ratio is lower than or equal to 0.1.  
 7 This discrete procedure can be generalized in a continuum way considering plane flexo-compression according to Fig. 7.  
 8 Then:

$$GSF_i = \frac{1}{2} \frac{h_i}{e_i} \quad GSF_i = \frac{1}{1 - \frac{2}{3} \alpha_i} \quad (6)$$

10 where  $\alpha_i$  is the ratio between the compressed area and the whole area of the contact surface.

11 Finally, the geometrical factor of safety of the whole structure  $GSF_{str}$  is equal to the minimum value along the analyzed  
 12 joints:

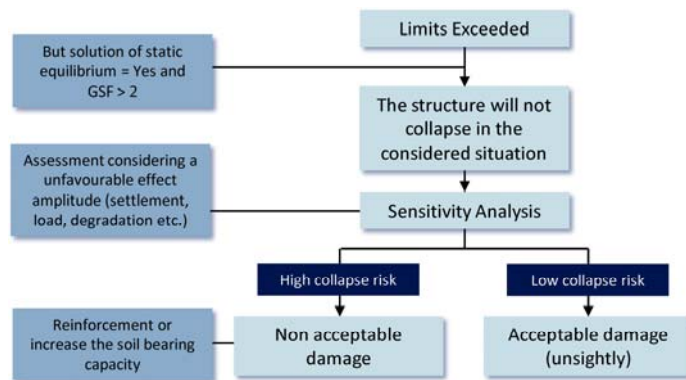
$$GSF_{str} = \min(GSF_i) \quad (7)$$



15  
 16 **Fig. 7.** The relationship between the thrust line and the contact pressure at the bed joints

17  
 18 The ultimate limit state of SEQ considering the sliding between blocks is also checked obtaining a static equilibrium  
 19 solution in all of the design situations calculated with Abaqus [28]. This work proposes a partial factor  $\gamma_R=3$  for decrease  
 20 the characteristic value of the static friction coefficient considered at the bed joints ( $\mu_k=0.6$  for the Saint Sebastian church)  
 21 in order to check this ultimate limit state taking into account the high uncertainty in both the material properties and the  
 22 quality of the building execution that affects to the sliding resistance. The proposed value for this partial factor is focused  
 23 on guaranty the same structural reliability level checking both the ultimate limit state of SEQ considering the sliding  
 24 between blocks and the ultimate limit state of STR. In fact, both the sliding between blocks and the masonry strength are

1 the basis of the masonry failure criteria of Mann & Müller [35], and they depend on the material properties uncertainties,  
 2 considered with the partial factor  $\gamma_R=3$  recommended by the Eurocode 6 [32] for a masonry structures composed by stone  
 3 blocks and bed joints of poor mortar.  
 4 The ultimate limit state of STR is checked comparing the maximum value of the compressive stress field with the design  
 5 value of the masonry compressive strength ( $f_d$ ) and the maximum value of tensile stress field with the design value of the  
 6 blocks tensile strength ( $f_{b,td}$ ). If these limits are exceeded, the diagram shown in the Fig. 8 can be followed in order to  
 7 study the risk of the material damages in the structure.  
 8 The safety of the structure considering the active or passive reinforcement resistance, if it is installed, is checked  
 9 comparing the maximum value of tensile stress in the reinforcement with the design value of the reinforcement tensile  
 10 strength specified by the manufacturer under the Eurocodes criteria.  
 11 Finally, the ultimate limit state of the SBC is checked using the nodal reactions obtained at the bottom face of the FEM  
 12 model foundation in all of the analysed situations under the Eurocode 7 [40] criteria.  
 13



14  
 15 **Fig. 8** The assessment of masonry damages  
 16

17 **3. Results**

18 **3.1 Results for the original structure**

19 The deformed model shown in Fig. 9 is the static equilibrium solution when the self-weight of the structure and the  
 20 imposed loads due to the roof maintenance are applied on the model without foundation settlements considered. It can  
 21 be deduced from this result that the geometrical factor of safety of the portal frame is  $GSF \geq 3$ , because the contact area  
 22 ratio is  $A = 1$  at every joint, that is to say, the thrust line cross all bed joints through its section kern. Moreover, a static  
 23 equilibrium solution is obtained in all of the design situations, where neither sliding between pieces occurs and  
 24 therefore the assessed portal frame is reliable regarding to the ultimate limit state of SEQ considering both the structural  
 25 stability and the sliding between blocks.

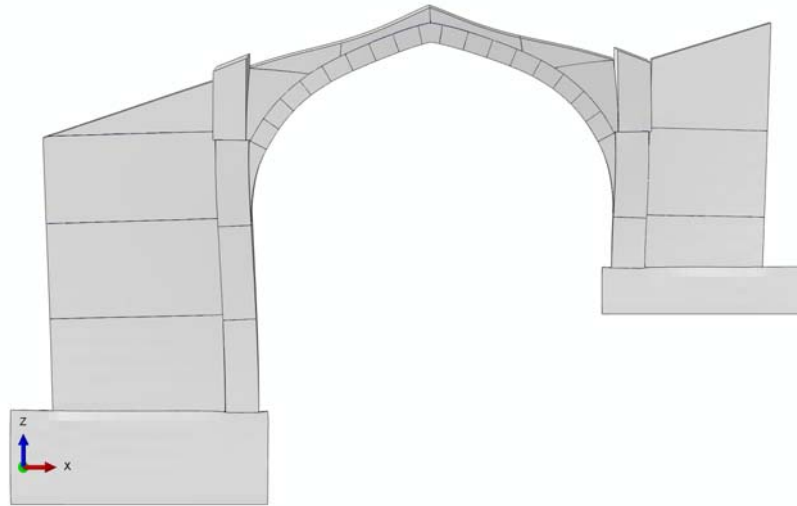


**Fig. 9.** Deformed model (2000 times extended) calculated without foundation settlements

The stress field of the calculated discontinuous FEM model applying the extreme combination of design actions for a persistent design situation without foundation settlements considered is shown in Fig. 10. Only compressive stress acts in the portal frame with a maximum value of 0.79 MPa. So, the masonry strength is 6.3 times higher than the maximum compressive stress and the portal frame is reliable regarding to the ultimate limit state of STR in this situation.

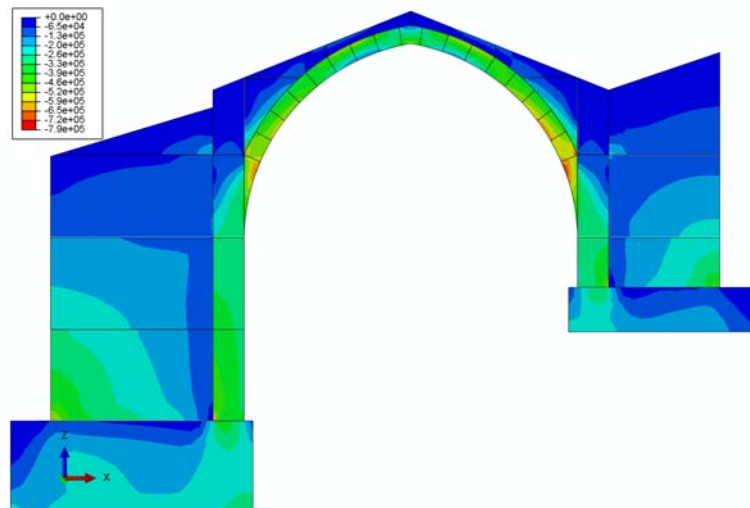
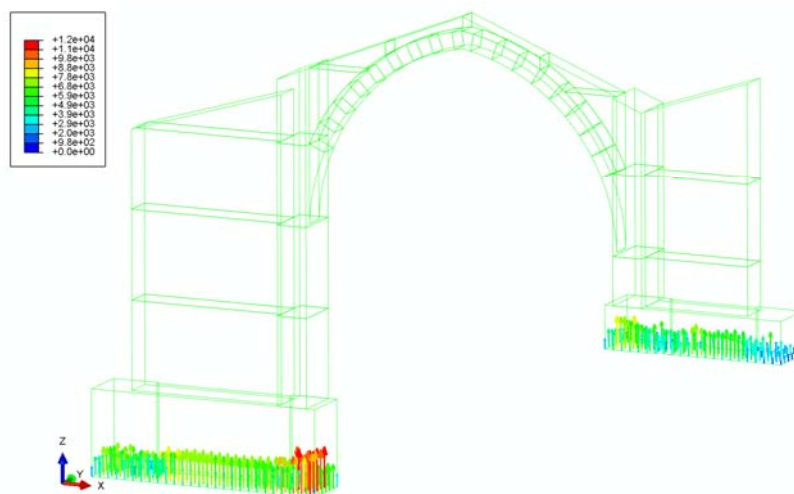


**Fig. 10** Stress field (in Pa) on the model calculated without foundation settlements

The nodal reactions at the base of the foundations are shown in Fig. 11. They are considered to determine the maximum and minimum values of the vertical pressure on the ground which are 0.3/0.1 MPa under the left foundation and 0.2/0.02 MPa under the right foundation, respectively. The soil bearing capacity is 0.3 MPa, according geotechnical studies, so the portal frame is also reliable regarding to the ultimate limit state of SBC in this situation.

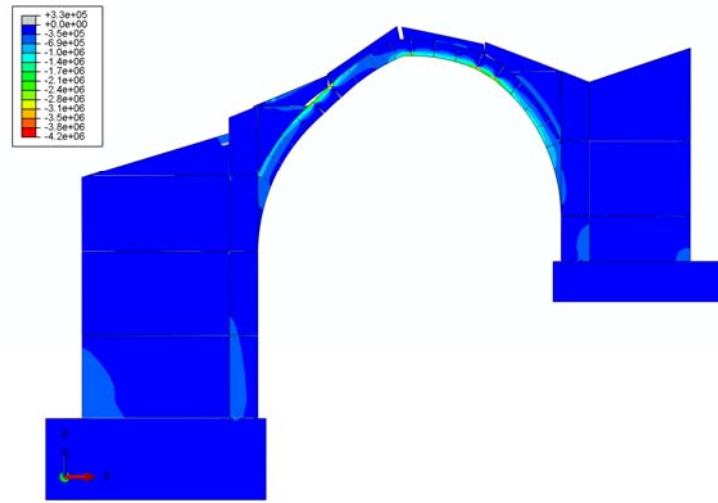
1 From the above results, it can be deduced that the settlement detected in the left foundation of the assessed portal frame  
 2 (Fig. 1) is due to a reduction of the soil bearing capacity by a water filtration from the waste water outlet or the excavation  
 3 done next to the affected foundation, but not due to an excessive foundation pressure.  
 4 Next, a new analysis considering an evolutionary settlement in the left foundation was performed. The left foundation was  
 5 lowered from its initial level position until 100 mm, in order to determine the value of the critical settlement where any  
 6 ultimate limit state (SEQ or STR) is exceeded and then, the reliability class of the portal frame would not be the RC3.  
 7 The stress field on the deformed model when the settlement is equal to 25 mm is shown in Fig. 12. Two cracked joints can  
 8 be seen in the arch, but they are two “hinging” joints which are necessary to adapt the portal frame to the new boundary  
 9 conditions, so the geometrical factor of safety ( $GSF \geq 3$ ) is not affected. Therefore, the portal frame is reliable in this new  
 10 situation regarding to the ultimate limit state of SEQ. A maximum compressive stress value of 4.2 MPa, lower than the  
 11 masonry compressive strength, and the ultimate limit state of STR is satisfied. That value is close to the masonry  
 12 compressive strength, so 25 mm should be approximately the critical value of the settlement in which the portal frame will  
 13 be in the limit of the masonry failure. On the other hand, masonry damages could appear when the settlement is increased  
 14 over 25 mm and the masonry will start to work under non linear behaviour.  
 15



16  
 17 **Fig. 11.** Nodal reactions (in N) at the base of the foundations of the model calculated without foundation settlements  
 18  
 19 The plastic strain field on the deformed model when the settlement is equal to 100 mm is shown in Fig. 13. Two cracked  
 20 joints can be seen in the arch of the FEM model, but this number is not enough to create a collapse mechanism. Therefore,  
 21 the portal frame is reliable in this situation for the ultimate limit state of SEQ, considering the structural stability and the  
 22 sliding between blocks, but it is not reliable considering the ultimate limit state of STR because there are two areas in the  
 23 FEM model that have suffered irreversible damages due to an excessive compressive stress. Then, the masonry will

1 failure according to the criterion III of Mann & Müller [15] (Fig. 5) if the foundation settlement is increased from 25 mm  
2 until 100 mm, decreasing its current reliability level.

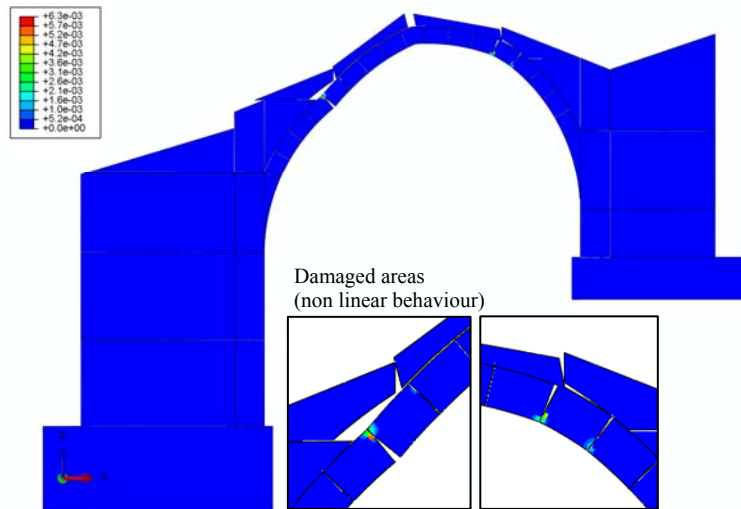
3



4

5 **Fig. 12.** Stress field (in Pa) on the deformed model (35 times extended) calculated considering a settlement of 25 mm

6



7

8 **Fig. 13.** Plastic strain field on the deformed model (10 times extended) calculated considering a settlement of 100 mm

9

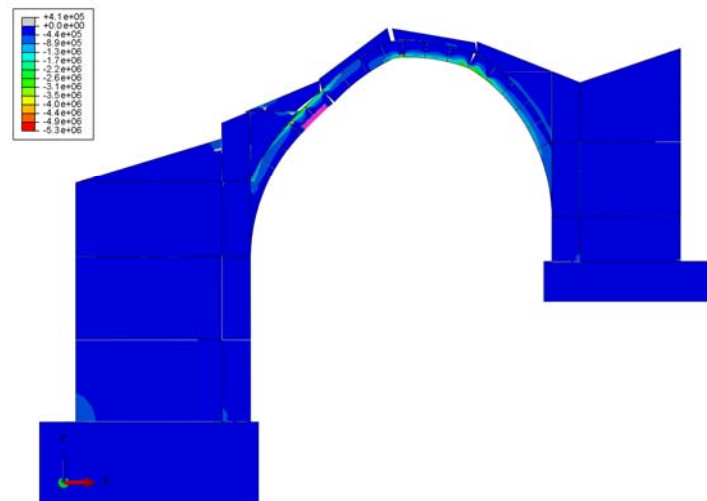
### 10 3.2 Results for the reinforced structure

11 Cracked joints were detected in the study “on site” of the Saint Sebastian church but without damages in the masonry.  
12 Therefore, it can be considered that the current foundation settlement is lower or equal to 25 mm and the structure can be  
13 considered as reliability class RC3.

14 If the settlement goes forward, the masonry resistance could be increased installing shells of steel or carbon fibre  
15 composite fixed with epoxy resin to the masonry structure at each cracked joint. The installation of these elements will

1 lock the opening of the cracked joints avoiding damages due to the increase of the local compressive stress. Figure 14  
2 shows the deformed model when the settlement is equal to 100 mm but two shells of steel of 5 mm thickness has been  
3 fixed at one cracked joint when the settlement was equal to 25 mm. In this case, the increase of the compressive stress at  
4 the cracked joint has been locked with the reinforcement installation but another cracked joint has appeared starting to  
5 work under a lower compressive stress with the forward of the foundation settlement. Therefore, the reinforcement  
6 installation delay the apparition of damages but, in this case, it will not be enough to avoid them if the settlement would  
7 be of 100 mm because the ultimate limit state of STR will be exceeded as can be seen in Fig. 15. Then, it will be also  
8 necessary to increase the soil bearing capacity with injections of cement or with grout under pressure in the terrain located  
9 below the affected foundation in order to stop its settlement before it exceeding 50 mm, or to install micropiles that will  
10 support the existing foundation at the affected area.

11



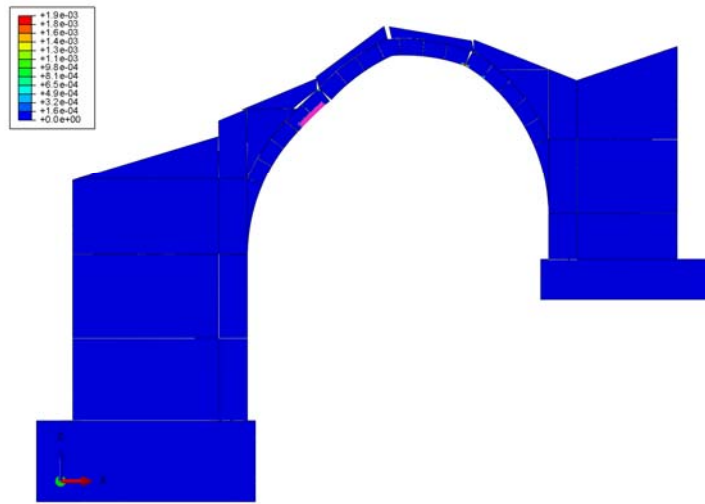
12

13 **Fig. 14.** Stress field (in Pa) on the deformed model (10 times extended) calculated considering a settlement of 100 mm  
14 and two steel shells installed when the settlement was 25 mm.

15

16 On the other hand, the installation of post tensioned tendons after drilling the masonry structure and fixing its ends with  
17 anchors could be done in order to avoid damages in the masonry if the foundation settlement exceeds 25 mm. Figure 16  
18 shows the deformed model when the settlement is equal to 100 mm but two prestressed tendons with a load of 20000 N  
19 are installed near the cracked joint when the settlement was equal to 25 mm. These active reinforcements close the  
20 cracked joint when they are installed but also forces the sliding and turning of the block in which they have been  
21 anchored. Therefore, the contact area between blocks is increased and the local compressive stress is decreased. But  
22 anyway, this solution presents the same problem than the exposed above, because another joint crack and damages will  
23 appear if the settlement would increase until 100 mm, as it is shown in the Fig. 17, so it will be also necessary to  
24 increase the soil bearing capacity or to install micropiles in this situation.





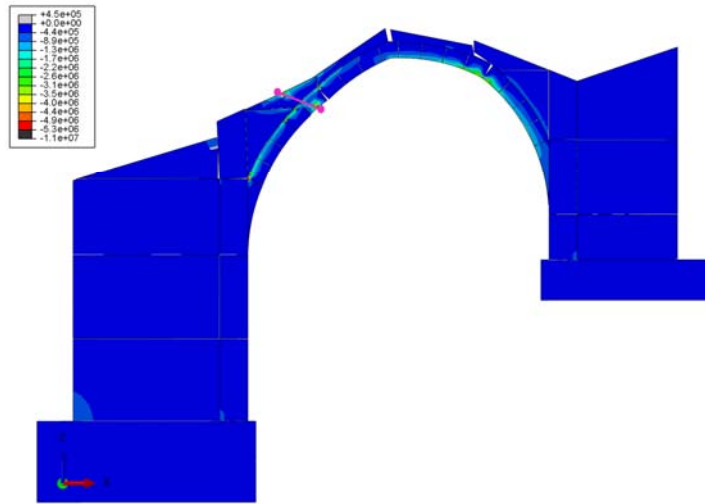
1

2

3

4

**Fig. 15.** Plastic strain field on the deformed model (10 times extended) calculated considering a settlement of 100 mm and two steel shells installed when the settlement was 25 mm.



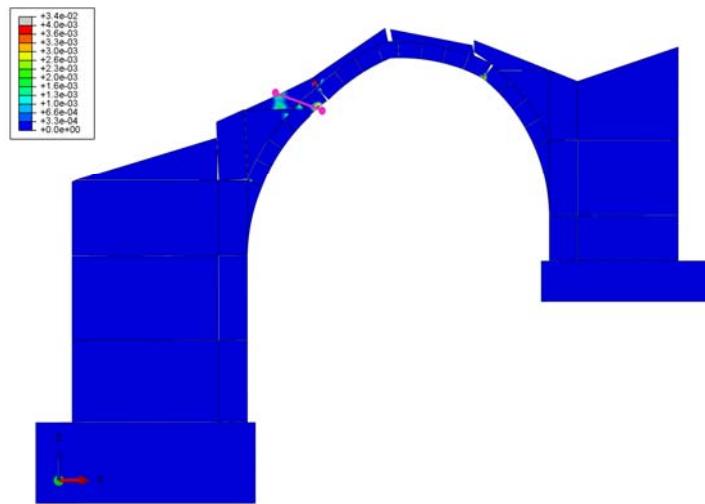
5

6

7

8

**Fig. 16.** Stress field (in Pa) on the deformed model (10 times extended) calculated considering a settlement of 100 mm and two posttensioned tendons installed when the settlement was 25 mm.



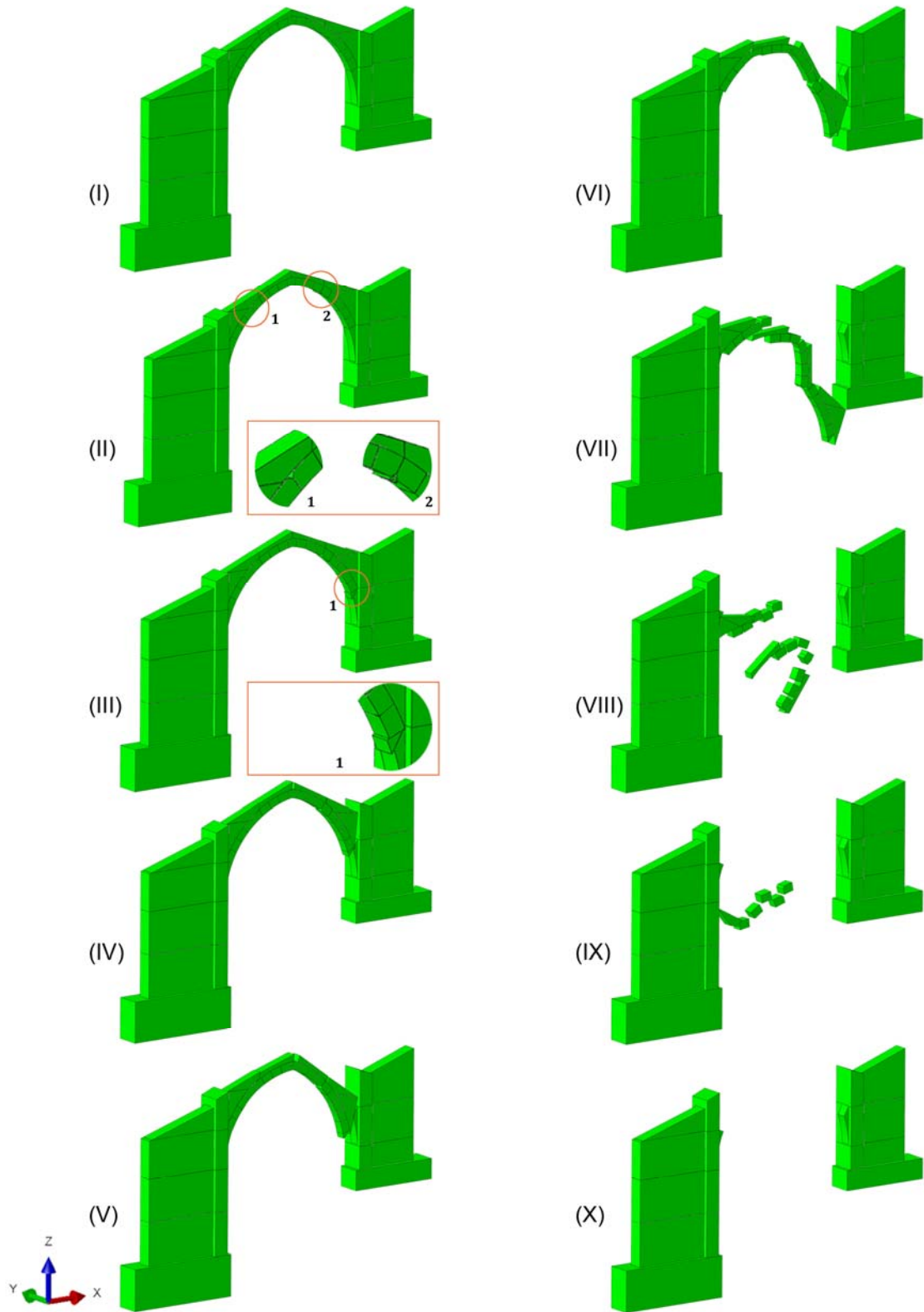
9

10

11

**Fig. 17.** Plastic strain field on the deformed model (10 times extended) calculated considering a settlement of 100 mm and two posttensioned tendons installed when the settlement was 25 mm.

1 Tables 3, 4 and 5 summarize the results obtained for different values of sandstone Young's modulus. According the  
2 results, the structural behaviour under settlements shows similar trends in every case, validating the reinforcement  
3 solutions analyzed. Finally, the collapse of the frame can be predicted by means of an evolutionary analysis. Figure 18  
4 shows the sequence representing such collapse.



5  
6 **Fig. 18.** Frame collapse for a settlement greater than 100 mm (sequential images).

1

**Table 3.** Results for different values of sandstone Young's modulus. Original structure

Sandstone Young's modulus (MPa)	Keystone displacement (mm)			Maximum compressive stress (MPa)			Maximum plastic strain		
	A (*)	B (**)	C (***)	A (*)	B (**)	C (***)	A (*)	B (**)	C (***)
<b>16000 (-20%)</b>	0.57	12.33	46.89	-0.79	-3.8	-5.0	0	0	0.0064
<b>20000</b>	0.45	12.14	46.69	-0.79	-4.2	-5.0	0	0	0.0063
<b>24000 (+20%)</b>	0.39	11.96	46.57	-0.79	-4.4	-5.0	0	0	0.0062

(\*) Without settlement; (\*\*) With a settlement of 25 mm; (\*\*\*) With a settlement of 100 mm

2

3

4

**Table 4.** Results for different values of sandstone Young's modulus. Structure reinforced with two steel shells

Sandstone Young's modulus (MPa)	Keystone displacement (mm)	Maximum compressive stress (MPa)	Maximum plastic strain
	Settlement of 100 mm	Settlement of 100 mm	Settlement of 100 mm
<b>16000 (-20%)</b>	46.05	-5.0	0.0020
<b>20000</b>	45.69	-5.0	0.0019
<b>24000 (+20%)</b>	45.45	-5.0	0.0018

5

6

**Table 5.** Results for different values of sandstone Young's modulus. Structure reinforced with two prestressed tendons

Sandstone Young's modulus (MPa)	Keystone displacement (mm)	Maximum compressive stress (MPa)	Maximum plastic strain
	Settlement of 100 mm	Settlement of 100 mm	Settlement of 100 mm
<b>16000 (-20%)</b>	51.25	-5.0	0.0434
<b>20000</b>	51.23	-5.0	0.0349
<b>24000 (+20%)</b>	51.07	-5.0	0.0289

7

#### 4. Discussion

8

9

10

11

12

13

14

15

16

17

The methodology proposed in this paper for the assessment of masonry historical structures according to Eurocodes is based on the analysis of a discontinuous MEF model with Abaqus, which allows checking all the ultimate limit states in any design situation. The method considers both the modern reliability criterion of the Eurocodes (the limit state method with the partial factors) and the classical approach of the Limit Analysis (the geometrical factor of safety) in the same procedure and using only one FEM model, which is not considered by another FEM approaches like macro or micro-models. The geometrical factor of safety is important to check the ultimate limit state of SEQ taking into account the high uncertainty regarding the high execution tolerances existing in this type of structure and that are not considered in the FEM model. Obviously, this factor could not be necessary if the local and global imperfections were represented in the geometric model shape (but it is very difficult to achieve) or if partial factors were applied to the stabiliser and destabiliser

1 actions (but it is impossible because in this type of structures these actions are mainly the same, the self-weight of the  
2 structure).

3 On the other hand, the proposed methodology has the following advantages over the Limit Analysis (any of them even  
4 over another FEM approaches besides the calculation of the geometrical factor of safety):

- 5 • Addresses much more situations: It can consider foundation settlements, wear of blocks, different types of  
6 material behaviour, active or passive reinforcements as it is shown in the Figs. 14 and 16, joints sealing with non  
7 shrinkage grout, dynamic response in order to consider the effect of the seismic action and so on.
- 8 • Besides the ultimate limit state of SEQ considering the structural stability though the geometrical factor of  
9 safety, the proposed methodology allows to check ultimate limit state of SEQ considering the sliding between  
10 blocks, the ultimate limit state of STR and the ultimate limit state of the SBC.
- 11 • The collapse progress can be predicted in case that the structure loses the stability.

12 Due to the reasons exposed above, the methodology developed in this work represents a way for the assessment of  
13 historical monumental structures in order to check their ultimate limit states according to the Eurocodes. In fact, it has  
14 been applied to assess the Saint Sebastian church located in Piedratajada (Zaragoza, Spain) obtaining the following  
15 conclusions:

- 16 • From the point of view of its design, the reliability level of the masonry structure is higher than the limit required  
17 by the Eurocodes (considering the SEQ, STR and SBC ultimate limit states).
- 18 • In the current situation (an approximately 25 mm of foundation settlement has appeared), the reliability level of  
19 the masonry structure is next to the limit that the Eurocodes accepts. In fact, damages could start to appear if the  
20 settlement goes forward.
- 21 • In the situation of the settlement foundation goes forward, an active or passive reinforcement can be installed, but  
22 it only delays the possibility that damages appear in the structure, delaying them until a settlement of 50 mm  
23 instead of 25 mm.
- 24 • The most efficient solution is, in case of the settlement goes forward (that will be controlled by tests), is to  
25 increase the soil bearing capacity with injections of cement or with grout under pressure in the terrain located  
26 below the affected foundation in order to stop it, or to install micropiles that support the existing foundation at  
27 the affected area.

1 Despite the performed analyses with different Young's modulus values, a limitation of the study concerns material  
2 properties. So, although different Young's modulus values have been considered in the range proposed by different  
3 authors, verifying the effect on the structural behaviour, compression tests on block specimens in order to assess their  
4 compressive strength and Young's modulus should be done for future studies.

## 6 **References**

- 7 [1] Heyman, J. The stone skeleton: Structural engineering of masonry architecture. Cambridge University Press  
8 1995.
- 9 [2] Heyman, J. Basic structural theory. Cambridge University Press 2008.
- 10 [3] Benedetti A, Steli E. Analytical models for shear–displacement curves of unreinforced and FRP reinforced  
11 masonry panels. *Construction and Building Materials* 2008; 22: 175–185.  
12 doi:10.1016/j.conbuildmat.2006.09.005.
- 13 [4] Lourenco PB, Rots JG. Multisurface interface model for analysis of masonry structures. *Journal of Engineering*  
14 *Mechanics* 1997; July: 660-668.
- 15 [5] Dhanasekar M, Haider W. Explicit finite element analysis of lightly reinforced masonry shear walls. *Computers*  
16 *and Structures* 2008; 86: 15–26. doi:10.1016/j.compstruc.2007.06.006.
- 17 [6] Giordano A, Mele E, De Luca A. Modelling of historical masonry structures: comparison of different approaches  
18 through a case study. *Engineering Structures* 2002; 24: 1057–1069.
- 19 [7] Kishi Y, Nozaka K, Izuno K. Dynamic behavior of multi-span masonry arch bridge using different stiffness in  
20 tension and compression. *Proceedings of the 8th International Conference on Structural Dynamics, EUROLYN*  
21 2011. ISBN 978-90-760-1931-4.
- 22 [8] Binda L, Modena C, Baronio G, Abbaneo S. Repair and investigation techniques for stone masonry walls.  
23 *Construction and Building Materials* 1997; 11(3): 133-142.
- 24 [9] Corradi M, Borri A, Vignoli A. Experimental study on the determination of strength of masonry walls.  
25 *Construction and Building Materials* 2003; 17: 325–337. doi:10.1016/S0950-0618(03)00007-2.
- 26 [10] Ercan E, Nuhoglu A. Identification of Historical Veziragasi Aqueduct Using the Operational Modal Analysis.  
27 *The Scientific World Journal* 2014; 2014: 1- 8. doi.org/10.1155/2014/518608.
- 28 [11] Betti M, Galano L. Seismic Analysis of Historic Masonry Buildings: The Vicarious Palace in Pescia (Italy).  
29 *Buildings* 2012; 2: 63-82. doi:10.3390/buildings2020063.
- 30 [12] Castellazzi G, Gentilini C, Nobile L. Seismic Vulnerability Assessment of a Historical Church: Limit Analysis  
31 and Nonlinear Finite Element Analysis 2013; Article ID 517454: 1- 12. doi.org/10.1155/2013/517454.
- 32 [13] Corradi M, Borri A, Vignoli A. Strengthening techniques tested on masonry structures struck by the Umbria–  
33 Marche earthquake of 1997–1998. *Construction and Building Materials* 2002; 16: 229–239.
- 34 [14] De Luca A, Giordano A, Mele E. A simplified procedure for assessing the seismic capacity of masonry arches.  
35 *Engineering Structures* 2004; 26: 1915–1929. doi:10.1016/j.engstruct.2004.07.003.
- 36 [15] Mallardo V, Malvezzi R, Milani E, Milani G. Seismic vulnerability of historical masonry buildings: A case study  
37 in Ferrara. *Engineering Structures* 2008; 30: 2223–2241. doi:10.1016/j.engstruct.2007.11.006.
- 38 [16] Modena C, Valluzzi MR, Tongini Folli R, Binda L. Design choices and intervention techniques for repairing and  
39 strengthening of the Monza cathedral bell-tower. *Construction and Building Materials* 2002; 16: 385–395.
- 40 [17] Valluzzi MR, Binda L, Modena C. Mechanical behaviour of historic masonry structures strengthened by bed  
41 joints structural repointing. *Construction and Building Materials* 2005; 19: 63–73.  
42 doi:10.1016/j.conbuildmat.2004.04.036.

- 1 [18] Roca P, Cervera M, Gariup G, Pela' L. Structural Analysis of Masonry Historical Constructions. Classical and  
2 Advanced Approaches. Arch Comput Methods Eng 2010; 17: 299–325. doi: 10.1007/s11831-010-9046-1.
- 3 [19] Massanas M, Roca P, Cervera M, Arun G. Structural analysis of Küçük Ayasofya Mosque in Istanbul. In:  
4 Structural Analysis of Historical Constructions IV. Balkema, Amsterdam. 2004.
- 5 [20] Lourenço PB. Computational strategies for masonry structures. PhD Thesis. Delft University of Technology,  
6 Delft, The Netherlands. 1996.
- 7 [21] Del Coz, JJ, García-Nieto PJ, Martínez-Luengas AL, Álvarez FP. Evaluation of the damage in the vault and  
8 portico of the pre-Romanesque chapel of San Salvador de Valdediós using frictional contacts and the finite-  
9 element method. International Journal of Computer Mathematics 2007; 84(3): 377-393  
10 [doi:10.1080/00207160701199757].
- 11 [22] Betti M., Vignoli A. Modelling and analysis of a Romanesque church under earthquake loading: assessment of  
12 seismic resistance. Engineering Structures 2008; 30(2): 352-367 [doi:10.1016/j.engstruct.2007.03.027].
- 13 [23] Romera LE, Hernandez S, Reinoso JM. Numerical characterization of the structural behaviour of the Basilica of  
14 Pilar in Zaragoza (Spain). Part 1: global and local models. Advances in Engineering Software 2008; 39:301-14  
15 [doi:10.1016/j.advengsoft.2007.01.009].
- 16 [24] Romera LE, Hernandez S, Reinoso JM. Numerical characterization of the structural behaviour of the Basilica of  
17 Pilar in Zaragoza (Spain). Part 2: constructive process effects. Advances in Engineering Software 2008; 39:315-  
18 26 [doi:10.1016/j.advengsoft.2007.01.008].
- 19 [25] Ivorra S, Pallares FJ, Adam JA, Tomas T. An evaluation of the incidence of soil subsidence on the dynamic  
20 behaviour of a Gothic bell tower. Engineering Structures 2010; 32(8): 2318-25  
21 [doi:10.1016/j.engstruct.2010.04.007].
- 22 [26] Betti M., Vignoli A. Numerical Assessment of the Static and Seismic Behaviour of the Basilica of Santa Maria  
23 all'Impruneta (Italy). Construction and Building Materials 2011; 25(12): 4308-4324  
24 [doi:10.1016/j.conbuildmat.2010.12.028].
- 25 [27] Ayensa A, Beltrán B, Ibarz E, Gracia L. A methodology for the assessment of historical structures based on  
26 finite element models. Journal of Heritage Conservation 2012; 32: 94-99.
- 27 [28] Dassault Systèmes [<http://www.3ds.com/>], 2014.
- 28 [29] Baker I. A treatise of masonry construction. J. Wiley & Sons, London. 1914.
- 29 [30] Union International des Chemins de Fer. Code UIC 778-3: Recommendations pour l'évaluation de la capacité  
30 portante des ponts-voûtes existants en maçonnerie et béton. UIC, 1995.
- 31 [31] Oliveira DV, Lourenço PB, Roca P. Cyclic behaviour of stone and brick masonry under uniaxial compressive  
32 loading. Materials and Structures 2006; 39(2): 247-257 [doi: 10.1617/s11527-005-9050-3]
- 33 [32] European Committee for Standardization. Eurocode 6: Design of masonry structures: EN 1996, CEN. 2005.
- 34 [33] Riddington JR, Ghazali MZ. Hypothesis for shear failure in masonry joints. Proceedings of the institution of civil  
35 engineers, 1989.
- 36 [34] Ohler A. Zur berechnung der druckfestigkeit von mauerwerk unter berucksichtigung der mehrachsigen  
37 spannungszustande in stein und mörtel. Bautechnik, Deutschland. 1986.
- 38 [35] Mann W, Müller H. Failure of shear-stressed masonry – An enlarged theory, tests and application to shear-walls.  
39 Proc. of the International Symposium on Loadbearing Brickwork, London. 1980
- 40 [36] European Committee for Standardization. Eurocode 1: Actions on structures: EN 1991, CEN. 2005.
- 41 [37] European Committee for Standardization. Eurocode 0: Basis of structural design: EN 1990, CEN. 2005.
- 42 [38] Lemaire M. Structural reliability. Iste Ltd. 2009

- 1 [39] Tichý M. Applied methods of structural reliability. Kluwer Academic Publishers. 1993
- 2 [40] European Committee for Standardization. Eurocode 7: Geotechnical design: EN 1997, CEN. 2005.